

## Supplementary information for

### Size selection and thin-film assembly of MoS<sub>2</sub> elucidates thousandfold conductivity enhancement in few-layer nanosheet networks

Sean P. Ogilvie,<sup>\*a</sup> Matthew J. Large,<sup>a</sup> Hannah J. Wood,<sup>a</sup> Aline Amorim Graf,<sup>a</sup> Frank Lee,<sup>a</sup> Jonathan P. Salvage,<sup>b</sup> Alice A. K. King<sup>a</sup> and Alan B. Dalton<sup>\*a</sup>

<sup>a</sup> University of Sussex, Brighton, BN1 9RH, UK

<sup>b</sup> University of Brighton, Brighton, BN2 4GJ, UK

\* [s.ogilvie@sussex.ac.uk](mailto:s.ogilvie@sussex.ac.uk); [a.b.dalton@sussex.ac.uk](mailto:a.b.dalton@sussex.ac.uk)

#### 1. Methods

##### 1.1 Exfoliation

MoS<sub>2</sub> powder, solvents and surfactants was purchased from Sigma Aldrich. MoS<sub>2</sub> was subjected to an initial sonication-centrifugation step to remove impurities and very small nanosheets; the bulk powder was added to 30 mL of cyclopentanone (CPO) at an initial concentration of 25 g/L and sonicated using a Sonic Vibra-cell VCX130 at 60% amplitude for 1 hour under ice bath cooling. The dispersion was centrifuged using a Thermo Scientific Sorvall Legend X1 with High Conic II rotor at 5000g for 5 mins; the supernatant containing the impurities and very small nanosheets was the discarded and the sediment was redispersed into 30 mL of fresh CPO. The redispersed sediment was subsequently sonicated at 60% amplitude for a further 3 hours under ice bath cooling.

Standard single-centrifugation-step dispersions, required for dense-packed film formation for conductivity measurements, were prepared by centrifugation at 5000g for 5 mins with the sediment discarded and the supernatant collected. This size selection typically yields dispersions of nanosheets with  $\langle N \rangle < 10$ , as confirmed by spectroscopic metrics by UV-visible extinction spectroscopy using a Shimadzu UV3600Plus spectrometer (Figure 1e in main text). Extinction spectroscopy was also used in conjunction with previously measured extinction coefficients to determine concentration of these dispersions, typically ~0.1 g/L.

Samples for spectroscopic studies were prepared by liquid cascade centrifugation at 5000 g with sediments collected and supernatants subjected to the subsequent step at the following times: 2, 4, 8, 16 and 32 mins. Dispersions were diluted to suitable concentrations and characterised by UV-visible extinction spectroscopy using a Shimadzu UV3600Plus spectrometer in quartz cuvettes with CPO reference sample. Established UV-visible spectroscopic metrics give average lateral sizes for the size-selected series as 355, 327, 269, 256 and 196 nm respectively.

Samples for non-Langmuir deposition techniques were prepared using the same procedure as for the CPO exfoliation but instead using NMP or aqueous Triton X-100 solution (0.25 g/L) as the dispersant. NMP-exfoliated MoS<sub>2</sub> was deposited by vacuum filtration onto nylon filter membranes with 25 nm pore size and allowed to dry before painting silver electrodes for conductivity measurement and surfactant-exfoliated MoS<sub>2</sub> was deposited by spray deposition using a standard airbrush onto microscope slides with sputtered gold electrodes.

Samples for size-dependent conductivity measurement were exfoliated by high-pressure homogenisation as described in our previous work.<sup>1,2</sup> Liquid cascade centrifugation was performed on surfactant-exfoliated MoS<sub>2</sub> dispersions at 3000 *g* with unexfoliated material discarded after 9 min centrifugation and sediments collected after centrifugation for 12 min, 14 min, 20 min, 40 min, 1 h, 2 h, 4 h, 8 h, and 12 h and redispersed into fresh 0.5 g/L surfactant solution with the supernatant collected for the subsequent centrifugation step. The average nanosheet length  $\langle L \rangle$  was measured using the spectroscopic metric. Samples were deposited by vacuum filtration as described above.

## 1.2 Raman spectroscopy

Standard single-centrifugation-step dispersions in CPO were characterised by Raman spectroscopy using a inVia Raman microscope with 660 nm excitation using a x50 objective, using previously-developed metrics and mapping approach.<sup>2</sup> This analysis, illustrated in Figure S1, yields histograms of pixel layer number and length. For these standard dispersions, this gives an average layer number of 5.7 monolayers and average nanosheet length of 89 nm.

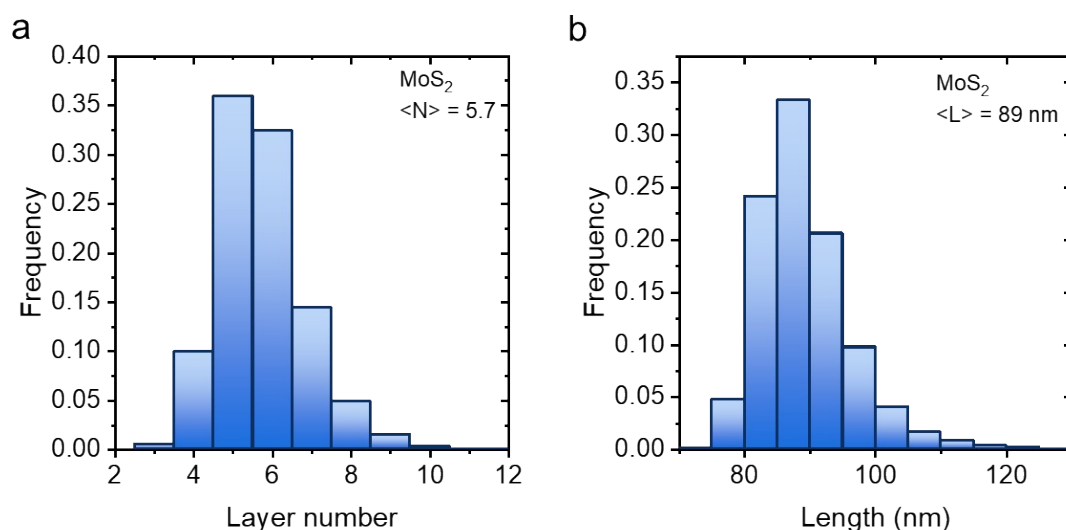


Figure S1: Histograms of (a) layer number and (b) length from Raman metric mapping analysis of CPO-exfoliated MoS<sub>2</sub> nanosheets.

## 1.3 Langmuir deposition

Dispersions were prepared at or diluted to concentrations below 0.1 g/L for thin-film assembly. Langmuir deposition was performed with a NIMA 102A Langmuir trough equipped with a platinum Wilhelmy plate with subphase area  $\sim 75$  cm<sup>2</sup> and a transparent window to allow mounting on a Leica spotting microscope to allow monitoring of film formation at 10x and 30x magnification. Deposition of MoS<sub>2</sub> films was performed by drop-wise addition of the  $\sim 0.1$  g/L dispersion onto the water subphase with  $\sim 0.1$  mL deposited before cycling the barriers to homogenise the film before depositing more material and  $\sim 2$  mL of dispersion typically deposited to give high area coverage as confirmed by in situ optical microscopy after compression to 25 cm<sup>2</sup>. Samples were transferred onto glass microscope slides or PET by the Langmuir-Schaefer horizontal deposition technique.

## 1.4 Microscopic and electrical characterisation

Film morphology and sample thickness was characterised by AFM (Bruker Dimension Icon with ScanAsyst Air probes). Thickness of vacuum-filtered and spray-deposited films were measured by micrometer screw gauge and stylus profilometry respectively. Films were further characterised by SEM using a Zeiss SIGMA field emission gun scanning electron microscope with Zeiss in-lens secondary electron detector. The working conditions used were 1.0 kV accelerating voltage, 20  $\mu\text{m}$  aperture, and 2.8 mm working distance. Langmuir films were prepared as described above and deposited onto glass or PET substrates with 30 nm sputtered gold bar electrodes ( $l = 19\text{ mm}$ ,  $w = 25\text{ mm}$ ) with part of the electrode area masked with Scotch tape to allow direct contact for electrical measurements. Silver paint electrodes were applied to vacuum-filtered samples. I-V characteristics were measured with a Keithley 2600 sourcemeter with potential difference -20 to 20 V. Sheet resistance and film thickness were measured to determine conductivity.

## 2. Solvent selection

CPO was initially identified as a promising candidate for single-solvent exfoliation and Langmuir deposition of liquid-exfoliated nanosheets through analysis of surface energy and Hansen solubility parameter matching to layered materials. Figure S2 shows the surface energy mismatch and Hansen interaction radius for a range of solvents with  $\text{MoS}_2$  plotted as a function of their boiling point, which should ideally be low for efficient Langmuir deposition. CPO is the only solvent in the bottom-left quadrant of both plots, indicating potential for exfoliation and deposition, and is one of the only water-immiscible solvents identified as suitable for exfoliation.

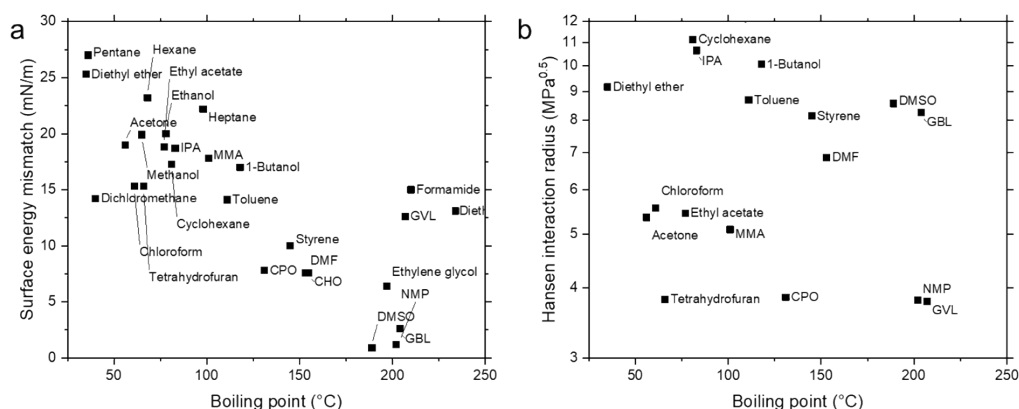


Figure S2: (a) Surface energy mismatch and (b) Hansen interaction radius for a range of solvent with  $\text{MoS}_2$  as a function of their boiling point, illustrating the selection criteria which identified CPO as ideal solvent for Langmuir deposition.

## 3. Solvatochromism

As discussed in the main text, Langmuir films are particularly interesting for spectroscopy, being sufficiently thin to allow simple transmission UV-visible spectroscopy on the same samples studied for electrical measurements, whereas other deposition techniques can require thicknesses which preclude transmission spectroscopy. This can be particularly important where spectroscopic measurements in dispersion can be affected by solvatochromic shifts due to the chemical

environment of the nanosheets. By performing UV-vis spectroscopy on dispersions and Langmuir films thereof, differences between the spectra can be attributed to these solvatochromic effects. Notably as shown in Figure 1f in the main text, the A-exciton feature of some samples exhibit a net blueshift which would conventionally be associated with reduction in layer number which is clearly unphysical for nanosheets aggregating into films. Instead, this can be understood as the partial elimination of a solvatochromic redshift of the dispersed nanosheets, with ketone solvents known to result in redshifts of up to 16 meV of MoS<sub>2</sub> spectral features.<sup>3</sup> Such shifts are particular important when determining average nanosheet layer number from established spectroscopic metrics<sup>4</sup>, since the layer number decays exponentially with A-exciton energy;

$$\langle N \rangle = 2.3 \times 10^{36} \exp(-44.16 E_A)$$

Therefore any redshift  $\Delta(eV)$  results in multiplicative factor increase in layer number

$$\langle N \rangle / \langle N \rangle_0 \approx \exp(44.16 \Delta)$$

For the largest ~10 meV differences observed shown in Figure S3, this corresponds to a factor of ~1.5 increase in layer number, suggesting such metrics may be better applied to films in the absence of solvent. In addition, the potential of this approach for chemical sensing and doping analysis clearly warrants further investigation.

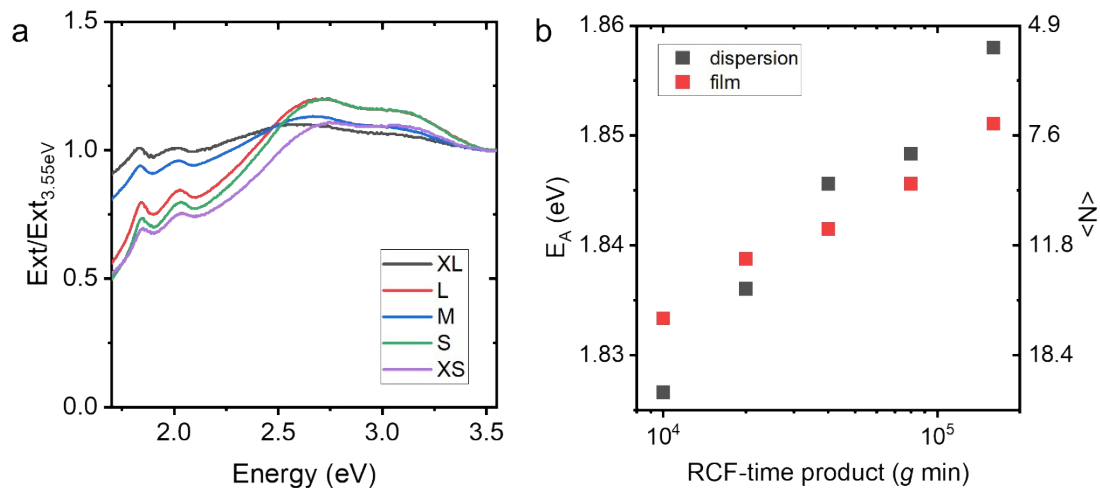


Figure S3: (a) UV-visible extinction spectra for Langmuir films corresponding to dispersions shown in Figure 1e and 1f in the main text. (b) A-exciton energy and corresponding layer number for dispersions and film as a function of relative centrifugal force-time product.

#### 4. I-V characteristics

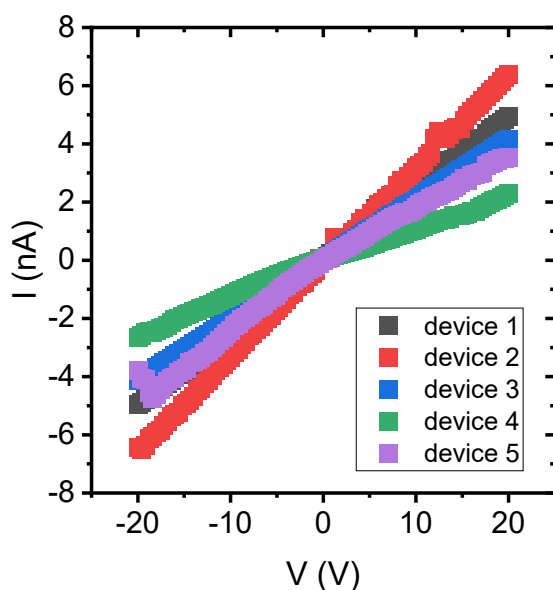


Figure S4: I-V characteristics for repeat Langmuir films ( $l/w \sim 1$ ) prepared under the same processing conditions yielding  $<100$  nm thickness, exhibiting  $<10$  G $\Omega$ /sq sheet resistance and corresponding conductivities around  $10^{-3}$  S/m.

#### References

- 1 M. J. Large, S. P. Ogilvie, A. A. Graf, P. J. Lynch, M. A. O'Mara, T. Waters, I. Jurewicz, J. P. Salvage and A. B. Dalton, *Adv. Mater. Technol.*, 2020, **5**, 2000284.
- 2 A. Amorim Graf, S. P. Ogilvie, H. J. Wood, C. J. Brown, M. Tripathi, A. A. K. King, A. B. Dalton and M. J. Large, *Chem. Mater.*, 2020, **32**, 6213–6221.
- 3 N. Mao, Y. Chen, D. Liu, J. Zhang and L. Xie, *Small*, 2013, **9**, 1312–1315.
- 4 C. Backes, R. J. Smith, N. McEvoy, N. C. Berner, D. McCloskey, H. C. Nerl, A. O'Neill, P. J. King, T. Higgins, D. Hanlon, N. Scheuschner, J. Maultzsch, L. Houben, G. S. Duesberg, J. F. Donegan, V. Nicolosi and J. N. Coleman, *Nat. Commun.*, 2014, **5**, 4576.